Progress In Electromagnetics Research C, Vol. 3, 129–142, 2008

MULTI-WAVELENGTHS OPTICAL SWITCHING AND TUNABLE FILTERS USING DYNAMIC SUPERIMPOSED PHOTOREFRACTIVE BRAGG GRATING

M. J. Moghimi and H. G. Fard

Faculty of Electrical Engineering
Amirkabir University of Technology
Tehran, Iran

A. Rostami

Photonics and Nanocrystal Research Lab.
Faculty of Electrical and Computer Engineering
University of Tabriz
Tabriz 51664, Iran

Abstract—We present a new scheme for all optical multi-wavelengths switching and filtering using photorefractive materials to route optical signals without converting to electronic state. For this purpose the photorefractive effect which is a nonlinear optical effect seen in certain crystals and other materials that respond to light by altering their refractive index is used. When a photorefractive material is illuminated by patterned command light of intensity $I(x)$, a dynamic superimposed Bragg grating can be obtained which is used for optical multi-wavelength switching and filtering purposes.

1. INTRODUCTION

Fast modulation and switching of optical signals are important functions in optical communication systems. Up to now, the switching burden in such systems has been laid almost entirely on electronics. In every switching node, optical signals are converted to electrical form (O/E conversion), buffered electronically, and subsequently forwarded to their next hop after being converted to optical form again (E/O conversion). Electronic switching is a mature and sophisticated technology that has been studied extensively. However, as the network

capacity increases, electronic switching nodes seem unable to keep up. Apart from that, electronic equipment is strongly dependent on the data rate and protocol, and thus, any system upgrade results in the addition and/or replacement of electronic switching equipment. If optical signals could be switched without conversion to electrical form, both of these drawbacks would be eliminated. This is the promise of optical switching. Some of the most popular applications of optical switches consist of optical cross-connects [1], optical Add/Drop multiplexing [2], optical signal monitoring [3], optical signal processing tasks [4–6]. Many schemes have been suggested for all optical switching, for example by using nonlinear loop mirror [7], nonlinear directional coupler [8], Liquid-crystal optical switches [9, 10], Semiconductor Optical Amplifier Switches (SOAs) [1, 11] and nonlinear grating [12]. In some of theses designs, such as SOAs or electro-optic switches still need electronic devices to operate.

Photorefractive crystals are materials in which the local refractive index is slightly changed by spatially modulated light intensity. Thus, photorefractive crystals can be used as an active or a passive optical element in optical information processing, optical communication and optical storage [13]. Photorefractive materials exhibit photoconductive and electro-optic behavior, and have the ability to detect the store spatial distributions of optical intensity in the form of spatial patterns of altered of refractive index [14]. When a photorefractive material is exposed to light, free charge carriers (electrons or holes) are generated by excitation from impurity energy levels to an energy band, at a rate proportional to the optical power. These carriers then diffuse away from the positions of high intensity where they were generated, leaving behind fixed charges of the opposite sign. The result is the creation of an inhomogeneous space-charge distribution that can remain in a period of time after the light is removed. This charge distribution creates an internal electric field pattern that modulates the local refractive index of the material by virtue of the (Pockels) electro-optic effect [15]. With the diffracted intensity of command beams applied to photorefractive material, dynamic Bragg grating can be realized. Diffracted intensity of command beams switches optical signals with modulating Bragg condition and refractive index.

Organization of the paper is as follows.

In Section 2 theory of photorefractive effect is explained. Optical and electrical properties of photorefractive materials are presented in Section 3. Mathematical background for introducing optical switching using photorefractive materials is presented in Section 4. In Section 5 simulation results are illustrated. Finally the paper ends with a short conclusion.

2. THEORY OF PHOTOREFRACTIVE EFFECT

Absorption of a photon at position x can removes an electron from the donor level to the conduction band. The rate of photo ionization $G(x)$ is proportional both to the optical intensity and to the density of unionized donors. Thus

$$G(x) = s\left(N_D - N_D^+\right) I(x), \tag{1}$$

where N_D, N_D^+ and s are density of donors, density of ionized donors and a constant known as the photoionization cross section respectively. Since nonuniform optical intensity $I(x)$ is applied to photorefractive media, thus generated and excited electrons will be nonuniform $n(x)$. As a result, electrons diffuse from locations of high concentrations to locations of low concentration. The electrons recombine at a rate $R(x)$ proportional to their density $n(x)$, and to the density of ionized donors (traps) N_D^+, so that

$$R(x) = \gamma_R n(x) N_D^+, \tag{2}$$

where γ_R is a constant. In equilibrium condition the rate of recombination must equal the rate of photoionization, $R(x) = G(x)$, so,

$$n(x) = \frac{s}{\gamma_R} \frac{N_D - N_D^+}{N_D^+} I(x), \tag{3}$$

Each photogenerated electron leaves behind a positive ionic charge. When the electron is trapped (recombines), its negative charge is deposited at a different site. As a result, a nonuniform space-charge distribution is formed. This nonuniform space charge generates a position-dependent electric field $E(x)$, which may be determined by observing that in steady state the drift and diffusion electric-current densities must be equal magnitude and opposite sign, so that total current density vanishes,

$$J = e\mu_e n(x) E(x) - k_B T \mu_e \frac{dn}{dx} = 0, \tag{4}$$

where μ_e is electron mobility, K_B is Boltzmann's constant, and T is the temperature. Thus

$$E(x) = \frac{k_B T}{e} \frac{1}{n(x)} \frac{dn}{dx}, \tag{5}$$

Since the material is electro-optic, the internal electric field $E(x)$ locally modifies the refractive index in accordance with

$$\Delta n(x) = -\frac{1}{2} n^3 r E(x), \tag{6}$$

where n and r are the appropriate values of refractive index and electro-optic coefficient for the material respectively.

Relation between the incident light intensity $I(x)$ and the resultant refractive index change $\Delta n(x)$ may readily be obtained if we assume that the ratio $(N_D/N_D^+ - 1)$ in Eq. (3) is approximately constant and independent of x. In that case $n(x)$ is proportional to $I(x)$, so that gives

$$E(x) = \frac{k_B T}{e} \frac{1}{I(x)} \frac{dI}{dx} \tag{7}$$

Finally, substituting this into Eq. (6), provides an expression for the position-dependent refractive index change as a function of intensity,

$$\Delta n(x) = -\frac{1}{2} n^3 r \frac{k_B T}{e} \frac{1}{I(x)} \frac{dI(x)}{dx} \tag{8}$$

So, using Eq. (8) and introducing appropriate position dependent light intensity, desired dynamic Bragg Grating can be obtained.

3. PHOTOREFRACTIVE MATERIALS

The photorefractive effect is a macroscopic phenomenon. The formation of a grating with significant efficiency requires the excitation and transport of a large number of charge carriers. Because of the need to absorb photons and to create carriers, the speed of the photorefractive effect is fundamentally limited by the rate of photon arrival. The photon-limited time for the index grating is [16]

$$t = \left(\frac{h\upsilon}{q}\right)\left(\frac{\lambda}{\Lambda}\right)\left(\frac{\gamma}{\alpha_p}\right)\frac{2}{\pi\eta I Q}, \tag{9}$$

where $h\upsilon, I, \gamma, \eta, \alpha_p$ and Q are photon energy, intensity of the light, coupling constant, quantum efficiency, photoexcitation absorption coefficient and figure-of-merit for photorefractive material respectively. Note that the time constant is directly proportional to the coupling constant and is inversely proportional to the light intensity.

Due to its excellent photorefractive properties, Lithium Niobate ($LiNbO_3$) has extensive applications in optical computing, image processing, phase conjugation and laser harden. Appropriate doped Fe:$LiNbO_3$ crystal with high diffractive efficiency and high sensitivity becomes the most promising candidate for digital data holographic storage application [17, 18]. However, both long response time and low ability of optical damage resistance are the main disadvantages of Fe:$LiNbO_3$ crystal. They can be overcome by doping with

damage-resistant dopants, such as $Zn^{+2}, Mg^{+2}, In^{+2}$ and Sc^{+2}. In $Zn{:}Fe{:}LiNbO_3$ crystal, Zn ions substitute for $[NbLi]^{+4}$ and form $[ZnLi]^{+4}$ [19, 20]. Compared with $Fe{:}LiNbO_3$ crystal, concentration decreasing of $NbLi^{+4}$ in $Zn{:}Fe{:}LiNbO_3$ crystal improves the ability of optical damage resistance and shortens the response time [21, 22]. Furthermore, the reduction treatment on the $Zn{:}Fe{:}LiNbO_3$ changes the concentrations of Fe^{+2}, Fe^{+3} and $[NvLi]^{+4}$ and improves its photorefractive properties [23, 24]. Potassium Niobate (KNbO3) is a well-known electro-optic material, which when doped with impurities that act as donors and acceptors the crystal becomes photorefractive [15, 25, 26].

Table 1. omparison of calculated time constants for some materials.

Materials	$\lambda(\mu m)$	$\Lambda(\mu m)$	$\alpha_p(cm^{-1})$	$\gamma(cm^{-1})$	$t(s)$
GaAs	1.06	1.0	1.2	0.4	45×10^{-6}
GaAs:Cr	1.06	1.1	4.0	0.6	31×10^{-6}
$BaTiO_3$	0.515	1.3	1.0	20.0	2×10^{-3}
BSO	0.568	23.0	0.13	10.0	2×10^{-3}
GaP	0.633	1.0	2.0	0.3	3×10^{-5}
SBN(undoped)	0.5145	2.0	0.1	7.0	5×10^{-3}
SBN:75:Cr	05145	9.83	0.6	9.1	2×10^{-4}

It should mention that t is time constant by using Eq. (9) and assuming a quantum efficiency of 100% and incident intensity $1\,\mathrm{W/cm^2}$.

Also, numbers of electro-optic polymers have been investigated to fabricate a high performance light modulator due to their advantages, such as large optical nonlinearity, fast response time, and low dielectric constants [27–31]. However several problems with electro-optic polymers remain such as unstable optical nonlinearity, insufficient transparency, weak mechanical properties, and controllability of refractive index. Extensive researches are continued about electro-optic crystals and polymers.

4. MATHEMATICAL BACKGROUND

For Dynamic Photorefractive Bragg grating the following proposal is considered. In this figure a thick substrate and a thin photorefractive material considered as optical switches and filters. In the proposed structure, when the photorefractive material is illuminated by command light of intensity $I(x)$, predefined wavelength reflected back

from the structure. Command light modifies the reflection coefficient and Bragg wavelength by its distribution intensity. For this structure the index of refraction generally can be explained as follows.

$$n(x) = n_{ave} + \Delta n(x) \tag{10}$$

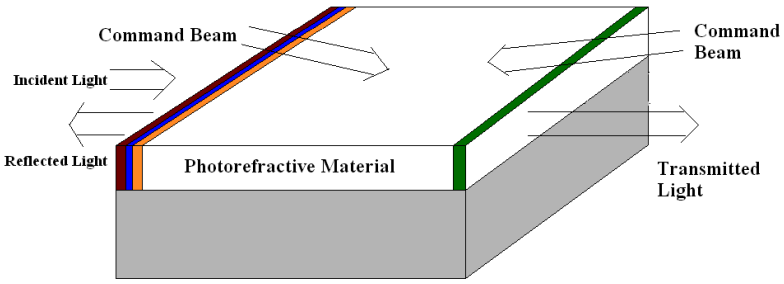

Figure 1. Schematic of the proposed photorefractive Bragg grating optical switch.

To analyze this structure, we divided it into N sections. Each section is considered homogenous. The approximated multilayer dielectric structure is described by

$$n(x) = \begin{cases} n_0 & x < x_0 \\ n_1 & x_0 < x < x_1 \\ n_2 & x_1 < x < x_2 \\ \cdot & \\ \cdot & \\ n_N & x_{N-1} < x < x_N \\ n_s & x_N < x \end{cases}, \tag{11}$$

where n_l is the refractive index of lth layer, x_l is the position of the interface between the lth layer and the $(l+1)$th layer, n_s is the substrate index of refraction and n_0 is refractive index of the incident medium respectively. The layer thicknesses d_i are L/N, where L is the length of the grating.

$$d_i = \frac{L}{N}, \qquad i = 1, 2, 3, \ldots, N \tag{12}$$

The electric field of a general plane-wave solution of the wave equation can be written as:

$$E = E(x)e^{i(\omega t - \beta z)}, \tag{13}$$

where the electric field distribution $E(x)$ can be written as:

$$E(x) = \begin{cases} A_0 e^{-ik_{0x}(x-x_0)} + B_0 e^{ik_{0x}(x-x_0)} & x < x_0 \\ A_l e^{-ik_{lx}(x-x_l)} + B_l e^{ik_{lx}(x-x_l)} & x_{l-1} < x < x_l \\ A_s e^{-ik_{sx}(x-x_N)} + B_s e^{ik_{sx}(x-x_N)} & x_N < x \end{cases}, \quad (14)$$

where k_{lx} is the x component of wave vectors and given as follows:

$$k_{lx} = \left[\left(\frac{n_l \omega}{c} \right)^2 - \beta^2 \right]^{\frac{1}{2}} \quad (15)$$

and is related to the ray angle θ_l by:

$$k_{lx} = n_l \frac{\omega}{c} \cos(\theta_l) = \frac{2\pi}{\lambda} \cos(\theta_l) \quad (16)$$

The electric field $E(x)$ consists of a right and left-traveling waves and can be defined by:

$$E_l(x) = Re^{-ik_l x} + Le^{ik_l x} = A_l(x) + B_l(x), \quad (17)$$

where $\pm k_l x, R$ and L are constants in homogenous layer. $E(x)$ is a continuous function of x. If we represent two amplitudes of $E(x)$ as column vectors, the column vectors are related by:

$$\begin{pmatrix} A_0 \\ B_0 \end{pmatrix} = D_0^{-1} D_l \begin{pmatrix} A_l \\ B_l \end{pmatrix} \quad (18)$$

$$\begin{pmatrix} A_l \\ B_l \end{pmatrix} = P_l D_l^{-1} D_{l+1} \begin{pmatrix} A_{l+1} \\ B_{l+1} \end{pmatrix} \quad (19)$$

where A_l and B_l represent the amplitude of plane waves at interface $x = x_l$ and D_l is dynamical matrix described by:

$$D_\alpha = \begin{pmatrix} 1 & 1 \\ n_\alpha \cos\theta_\alpha & -n_\alpha \cos\theta_\alpha \end{pmatrix}, \quad \alpha = 0, l, l+1 \quad (20)$$

where θ_α is the ray angle in each layer. P_l is propagation matrix and defined by:

$$P_l = \begin{pmatrix} e^{i\phi_l} & 0 \\ 0 & e^{-i\phi_l} \end{pmatrix} \quad (21)$$

$$\phi_l = k_{lx} \cdot d_l \quad (22)$$

The relation between A_0, B_0 and A_s, B_s (or A_{N+1}, B_{N+1}) can be determined by:

$$\begin{pmatrix} A_0 \\ B_0 \end{pmatrix} = \begin{pmatrix} M_{11} & M_{12} \\ M_{21} & M_{22} \end{pmatrix} \begin{pmatrix} A_s \\ B_s \end{pmatrix} \quad (23)$$

With the matrix given by:

$$\begin{pmatrix} M_{11} & M_{12} \\ M_{21} & M_{22} \end{pmatrix} = D_0^{-1} \left[\prod_{i=1}^{N} D_i P_i D_i^{-1} \right] D_s \tag{24}$$

This approach named Transfer Matrix Method (TMM) [32]. If the light is incident from medium 0, the reflection coefficient is defined as:

$$r(\lambda) = \left(\frac{B_0}{A_0} \right)_{B_s=0} \tag{25}$$

Similarly, the transmission coefficient is:

$$t(\lambda) = \left(\frac{A_s}{A_0} \right)_{B_s=0} \tag{26}$$

Using matrix equation (14) and definitions (15), (16), we obtain:

$$r(\lambda) = \frac{M_{21}}{M_{11}} \tag{27}$$

and

$$t(\lambda) = \frac{1}{M_{11}} \tag{28}$$

Also, the energy reflectance in the case of lossless medium is given by:

$$R(\lambda) = |r(\lambda)|^2 = \left| \frac{M_{21}}{M_{11}} \right|^2 \tag{29}$$

5. SIMULATION RESULTS AND DISCUSSION

All processes now use UV laser beams and side writing, the most popular one is described in Figure 2. The beam is focused onto the fiber through a pair of cylindrical lenses which shape the beam to a cross section of $15 \times 0.3\,\mathrm{mm}^2$ oriented along the length of the fiber. A second type of writing method is derived from photolithography using a phase mask made of silica glass (non-absorbing UV light). An excimer laser beam at normal incidence is modulated spatially by a phase mask grating. The diffracted light which forms a periodic, high contrast intensity pattern with half the phase mask grating pitch, photo imprints a refractive index modulation into the core of a photosensitive fiber placed behind, closely and parallel to the mask.

We consider an intensity distribution in the form of sinusoidal grating of period Λ, contrast m, and mean intensity I_0,

$$I(x) = I_0(1 + m\cos(2\pi x/\Lambda)) \tag{30}$$

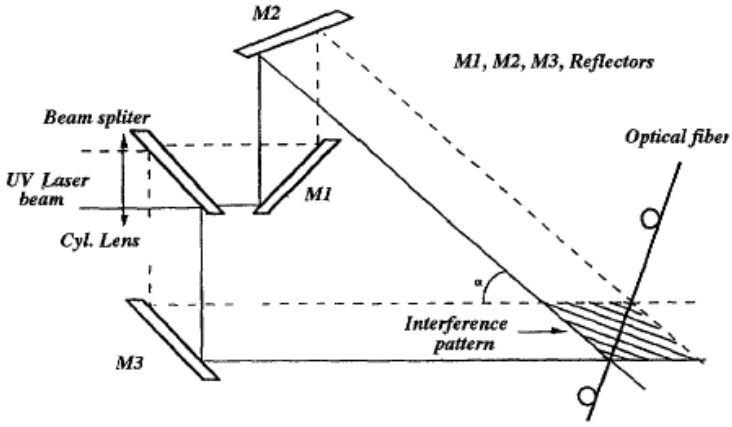

Figure 2. Apparatus set to write gratings in the core of optical fibers.

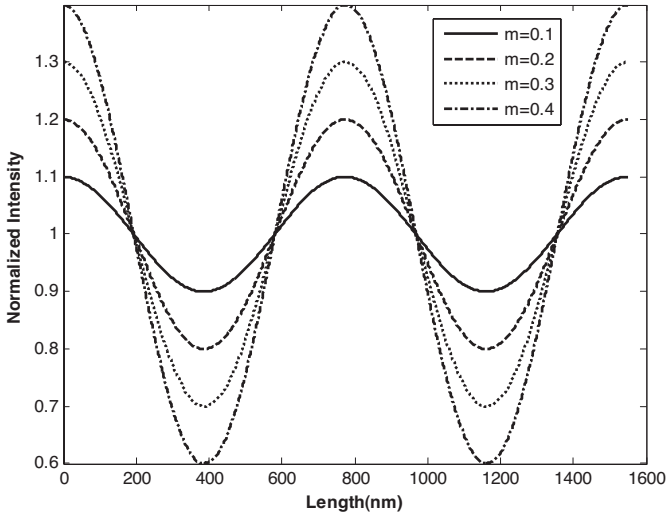

Figure 3. Normalized intensity (I/I_0) versus length for $\Lambda = 775$ (nm).

Fig. 3 shows normalized intensity (I/I_0) for different contrast.

By substituting Eq. (30) into Eq. (7) and Eq. (8), we obtain the internal electric field and refractive index distributions as follows,

$$E(x) = E_{Max}\frac{-\sin(2\pi x/\Lambda)}{1+m\cos(2\pi x/\Lambda)}, \tag{31}$$

$$\Delta n(x) = \Delta n_{Max} \frac{\sin(2\pi x/\Lambda)}{1 + m\cos(2\pi x/\Lambda)}, \tag{32}$$

where $E_{Max} = 2\pi(k_B T/e\Lambda)m$ and $\Delta n_{Max} = \frac{1}{2}n^3 r E_{Max}$ are the maximum values of $E(x)$ and $\Delta n(x)$, respectively. Δn_{Max} and E_{Max} for some photorefractive crystals are calculated in Table 2.

Table 2. Maximum electric field and refractive index variation in some photorefractive crystals for command light contrast $m = 1$ [33].

Materials	$\lambda(\mu m)$	$r(pm/V)$	n	Δn_{Max}	E_{Max}
$BaTio_3$	0.5	$r_{42} = 1640$	$n_e = 2.4$	3.700×10^{-3}	3.26×10^{5}
SBN	0.5	$r_{33} = 1340$	$n_e = 2.3$	2.700×10^{-3}	3.26×10^{5}
GaAs	1.1	$r_{12} = 1.43$	$n_e = 3.4$	4.173×10^{-6}	1.48×10^{5}
BSO	0.6	$r_{41} = 5$	$n = 2.54$	1.115×10^{-5}	2.72×10^{5}
$LiNbO_3$	0.6	$r_{33} = 31$	$n_e = 2.2$	4.493×10^{-5}	2.72×10^{5}
$LiTaO_3$	0.6	$r_{33} = 31$	$n_e = 2.2$	4.493×10^{-5}	2.72×10^{5}
$KNbO_3$	0.6	$r_{42} = 380$	$n = 2.3$	6.294×10^{-4}	2.72×10^{5}
GaP	0.56	$r_{41} = 1.07$	$n = 3.45$	6.408×10^{-6}	2.91×10^{5}

Fig. 4 shows how the contrast of command light modulates $\Delta n(x)$ and dynamic Bragg grating is realized.

Optical switching in dynamic Bragg grating schematically for typical parameters is depicted in Fig. 5. Since command light contrast

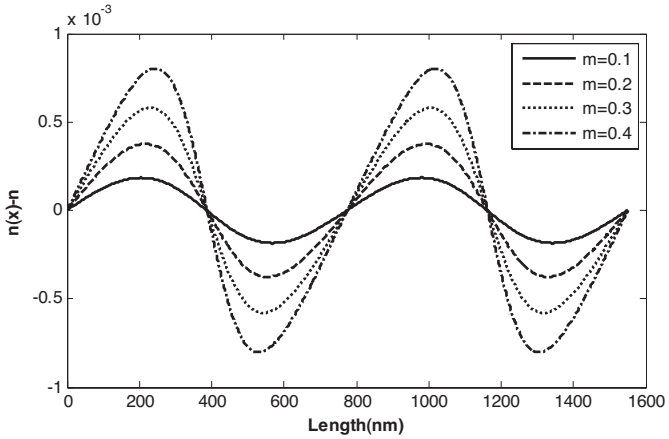

Figure 4. $\Delta n(x)$ versus grating length $\Lambda = 775$ (nm), $r = 100\,\mathrm{pm/V}$.

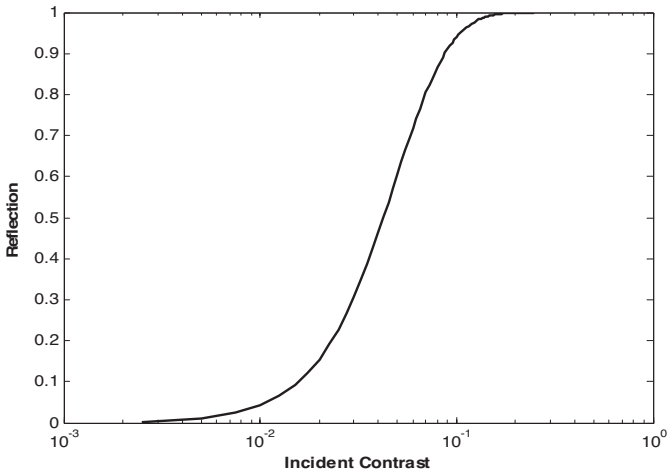

Figure 5. Reflection versus incident contrast for $L = 20\,\text{mm}$, $\Lambda = 775$ (nm), $r = 100\,\text{pm/V}$.

(m) modulates refractive index, reflection from device (Eq. (29)) changes.

Tunable optical filters based on dynamic Bragg grating is simulated in Fig. 6. Command light wavelength Λ tunes the transfer function of optical spectral filters by changing the Bragg condition ($\lambda_i = 2 \times \Lambda_i$).

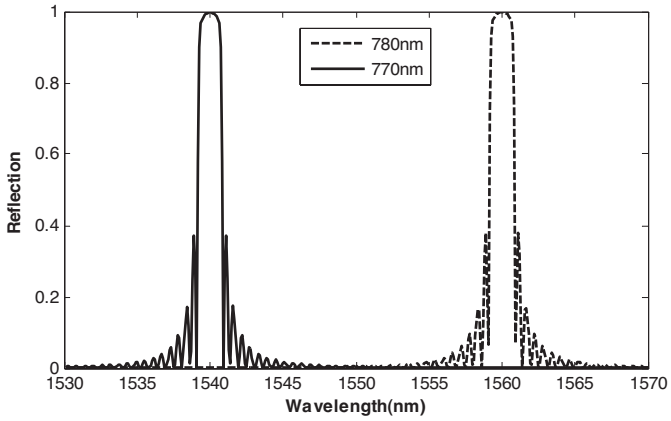

Figure 6. The reflection coefficient vs. wavelength $m = 0.5$, $L = 20\,\text{mm}$, $\Lambda = 770$ (nm), $\Lambda = 780$ (nm), $r = 100\,\text{pm/V}$.

As it was mentioned in introduction there are different alternatives for switching in electronic and optical domain [1–40]. But in this paper all-optical switching for single wavelength and multi-wavelength was considered.

By applying complex command light complex Bragg Gratings can be obtained and so the function such as filtering and switching operations can be realized simultaneously for multi wavelengths. One of interesting purpose is superimposed Bragg Gratings which can be implemented in the proposed structure.

6. CONCLUSION

In this paper photorefractive medium for realization of superimposed Bragg gratings for design of multi-wavelengths optical filters and switches has been presented and discussed. It was shown that all-optical dynamic Bragg grating can be implemented using the photorefractive materials. In this work typically optical switching and filtering have been reported.

REFERENCES

1. Ramaswami, R. and K. N. Sivarajan, *Optical Networks, a Practical Perspective*, Morgan Kaufmann, San Fransisco, CA, 1998.
2. Roberts, G. F., K. A. Williams, R. V. Penty, I. H. White, M. Glick, D. McAuley, D. J. Kang, and M. Blamire, "Monolithic 2×2 amplifying add/drop switch for optical local area networking," *ECOC '03*, Vol. 3, 736–737, Sept. 24, 2003.
3. Dugan, A., L. Lightworks, and J.-C. Chiao, "The optical switching spectrum: A primer on wavelength switching technologies," *Telecommunication Mag.*, May 2001.
4. Erdogan, T., "Fiber grating spectra," *J. Lightwave Technology*, Vol. 15, No. 8, Aug. 1997.
5. Zhao, J., X. Shen, and Y. Xia, "Beam splitting, combining, and cross coupling through multiple superimposed volume-index gratings," *Optics & Laser Technology*, Vol. 33, 23–28, 2001.
6. Hruschka, P. C., U. Barabas, and L. Gohler, *Optical Narrowband Filter without Resonances*, Ser.: ELEC. ENERG, Vol. 17, 209–217, 2004.
7. Doran, N. J. and D. Wood, *Opt. Lett.*, Vol. 13, 56, 1988.
8. Jensen, S. M., *IEEE J. Quantum Electron.*, Vol. QE-18, 1580, 1982.

9. De Dobbelaere, P., K. Falta, L. Fan, S. Gloeckner, and S. Patra, "Digital MEMS for optical switching," *IEEE Commun. Mag.*, 88–95, Mar. 2002.
10. Bregni, S., G. Guerra, and A. Pattavina, "State of the art of optical switching technology for all-optical networks," *Communications World. Rethymo*, WSES Press, Greece, 2001.
11. Mukherjee, B., *Optical Communication Networks*, McGraw Hill, New York, 1997.
12. Winful, H. G., J. H. Marburger, and E. Garmire, *Appl. Phys. Lett.*, Vol. 35, 379, 1979.
13. Yu, F. and S. Yin (eds.), *Photorefractive Optics*, Academic Press, San Diego, 2000.
14. Saleh, B. E. A. and M. C. Teich, *Fundamentals of Photonics*, John Wiley & Sons, 2003.
15. Gunter, P. and J. P. Huignard (eds.), *Photorefractive Materials and Their Applications II*, Springer-Verlag, New York, 1989.
16. Yeh, P., *Introduction to Photorefractive Nonlinear Optic*, John Wiley & Sons, 1993.
17. Burke, W. J., D. L. Staebler, W. Phillips, and G. A. Alphonse, *Opt. Eng.*, Vol. 17, 308, 1978.
18. Yang, C. H., Y. Q. Zhao, R. Wang, and M. H. Li, *Opt. Commun.*, Vol. 175, 247, 2000.
19. Zheng, W., N. D. Zhang, L. C. Zhao, et al., *Opt. Commun.*, Vol. 227, 259, 2003.
20. Zhen, X. H., L. C. Zhao, and Y. H. Xu, *Appl. Phys. B*, Vol. 76, 655, 2003.
21. Li, M. H., C. X. Liu, K. B. Xu, et al., *SPIE 2885*, 193, 1996.
22. Wu, Q., J. J. Xu, Q. Sun, et al., *Appl. Phys. Lett.*, Vol. 81, 4691, 2000.
23. Li, M. H., Q. Y. Zhao, K. B. Xu, et al., *Chin. Sci. Bull.*, Vol. 41, No. 8, 655, 1996.
24. Zhen, X. H., H. T. Li, Z. J. Sun, S. J. Ye, L. C. Zhao, and Y. H. Xu, *Mater. Lett.*, Vol. 58, 1000.1, 2004.
25. Reeves, R. J., M. G. Jani, B. Jassemnejad, R. C. Powell, G. J. Mizell, and W. Fay, *Phys. Rev. B*, Vol. 43, 71, 1991.
26. Medrano, C., M. Zgonik, I. Liakatas, and P. Günter, *J. Opt. Soc. Am. B*, Vol. 13, 2657, 1996.
27. Chelma, D. S. and J. Zyss, *Nonlinear Optical Properties of Organic Molecules and Crystals*, Vols. 1 and 2. Academic Press, New York, 1987.

28. Ulrich, D. R., *Nonlinear Optical and Electroactive Polymers*, P. N. Prasad (ed.), Plenum Press, New York/London, 1988.
29. Burland, D. M., R. D. Miller, C. A. Walsh, *Chem. Rev.*, Vol. 94, 31, 1994.
30. Dalton, L. R., A. H. Harper, R. Ghson, W. H. Steir, M. Ziari, H. Fetterman, Y. Shi, R. V. Mustacich, A. K.-Y. Jen, K. J. Shea, *Chem. Master.*, Vol. 7, 1060, 1995.
31. Dagni, R., *Chem. Eng. News*, Vol. 4, 22, March 1996.
32. Yeh, P., *Optical Waves in Layered Media*, John Wiley & Sons, 2005.
33. Yeh, P., "Fundamental limit of the speed of photorefractive effect and its impact on device applications and material research," *Appl. Opt.*, Vol. 26, 602–605, 1987.
34. Ghafoori-Fard, H., M. J. Moghimi, and A. Rostami, "Linear and nonlinear superimposed Bragg grating: A novel proposal for all-optical multi-wavelength filtering and switching," *Progress In Electromagnetics Research*, PIER 77, 243–266, 2007.
35. Sanyal, S. K., Q. M. Alfred, and T. Chakravarty, "A novel beam-switching algorithm for programmable phased array antenna," *Progress In Electromagnetics Research*, PIER 60, 187–196, 2006.
36. Aberg, I., "High-frequency switching and Kerr effect — Nonlinear problems solved with nonstationary time domain techniques," *Progress In Electromagnetics Research*, PIER 17, 185–235, 1997.
37. Mitilineos, S. A., C. A. Papagianni, G. I. Verikaki, and C. Capsalis, "Design of switched beam planar arrays using the method of genetic algorithms," *Progress In Electromagnetics Research*, PIER 46, 105–126, 2004.
38. Wei, W.-B., Q.-Z. Liu, Y.-Z. Yin, and H.-J. Zhou, "Reconfigurable microstrip patch antenna with switchable polarization," *Progress In Electromagnetics Research*, PIER 75, 63–68, 2007.
39. Afrang, S. and E. Abbaspour-Sani, "A low voltage MEMS structure for RF capacitive switches," *Progress In Electromagnetics Research*, PIER 65, 157–167, 2006.
40. Varlamos, P. K. and C. N. Capsalis, "Electronic beam steering using switched parasitic smart antenna arrays," *Progress In Electromagnetics Research*, PIER 36, 101–119, 2002.